

M. RZESZOTARSKA¹, I. KUNCE², D. ZASADA¹, M. POLAŃSKI^{1*}

FEASIBILITY STUDY OF METAL MATRIX COMPOSITE (IN625-WC) MANUFACTURING BY LASER ENGINEERED NET SHAPING (LENS®)

The present paper focuses on the technological approach to manufacturing composite in the form of Inconel 625 reinforced with tungsten carbide particles. Twenty-four samples with reinforcement amounts ranging from 30 to 90% (wt.%) and different numbers of deposited layers were manufactured with the use of Laser Engineered Net Shaping (LENS®). The metallurgical quality, microstructure, chemical and phase composition as well as hardness of the produced composites were determined. Digital microscopy, X-ray powder diffraction and SEM-EDS were employed for this purpose. Despite numerous cracks, the fabricated samples exhibited a greater hardness than single-layer coatings of analogous composition also produced by additive techniques. This phenomenon is likely a result of repeated crystallization of the composites in remelted areas. A dual mechanism of material strengthening is observed in the additively manufactured composites, both by the presence of reinforcing particles and precipitates of secondary phases.

Keywords: Metal matrix composite; ceramic reinforcement; additive manufacturing; direct laser deposition; Ni-based superalloy

1. Introduction

Nickel-based superalloys are used in applications requiring high strength, wear, fatigue and creep resistance, and corrosion resistance at elevated temperatures [1]. For example, they are used in the aerospace, marine and automotive industries [2]. Due to the limited machinability and energy consumption in the fabrication of Inconel 625 parts, the possibility of manufacturing these alloys using additive manufacturing techniques has been analyzed in recent years. The advantage of additive manufacturing (AM) techniques is the ability to create complex product geometries by “printing” the material layer by layer. Based on the type of raw material, AM processes can be classified as powder bed processes or so-called direct energy deposition (DED) processes involving direct feeding of powder or wire into the melting zone. The advantage of additive techniques using a high-energy laser beam and direct application of material through nozzles to a substrate is the possibility of in situ control of the chemical composition of the material to be deposited. In the process of material deposition, metal powders, ceramics, or alloy powders can be used, which allows the production of structural alloys, composites or functional materials, such as those with a gradient of chemical composition and properties. Control of the general

chemical composition of manufactured components is achieved by calibrating feed rates of various single-component or alloy powders. Achieving assumed chemical composition is more easily achieved if the feedstock powders have similar melting points and there is no risk of evaporation of the low-melting elements. Additive layer manufacturing processes, including direct energy deposition systems such as LENS®, can be considered repetitive welding processes, while subsequent weld layers can be used to construct 3D net or near-net shape components. Due to the high levels of residual stress, components produced by additive layer manufacturing processes often require heat treatment [3].

In the search for new materials with good mechanical properties and high wear resistance that can be produced by additive techniques, Inconel 625 is considered to be a matrix of composites due to its good weldability. Research on the possibility of manufacturing composites on the matrix of Inconel 625 by additive techniques involves reinforcement in the form of carbide particles such as WC, TiC, and SiC or ceramics such as Al₂O₃ [4]. In addition to increasing hardness and wear resistance, the use of a suitable reinforcing additive promotes uniform grain growth and reduces the anisotropy of mechanical properties compared to the formation of columnar dendritic structures that occur during rapid solidification in direct laser

¹ MILITARY UNIVERSITY OF TECHNOLOGY, FACULTY OF NEW TECHNOLOGIES AND CHEMISTRY, 01-476 WARSZAW, POLAND

² ROAD AND BRIDGE RESEARCH INSTITUTE, CORROSION AND CHEMISTRY DIVISION, 03-302 WARSZAW, POLAND

* Corresponding author: marek.polanski@wat.edu.pl



deposition of Inconel 625 [5,6] especially when additives are added as nanoparticles.

Among the types of reinforcement tested, liquid nickel has good wettability for WC particles, in addition to high hardness and high resistance to oxidation at elevated temperatures [7]. The possibility of applying additive techniques to the fabrication of Inconel 625-WC composites has been studied mostly with respect to coatings [8-11] in which the mass share of WC is usually up to 30% since bulk samples can be produced easily by sintering [6,12]. Due to the high-temperature gradient during additive manufacturing and partial dissolution of reinforcement particles, which leads to the formation of secondary carbides, Inconel 625-WC composites are prone to cracking. Attempts of additive manufacturing of bulk samples are limited to just a few layers of material [13,14].

The purpose of this study was to produce Inconel 625-WC composite samples in the form of both single coatings and bulk samples – up to 7 layers of material – with a uniform distribution of WC in the whole sample volume and with a controlled amount of reinforcing particles. In addition, composite samples were produced with an amount of reinforcing particles far greater than that reported in the literature concerning the fabrication of Inconel 625-WC composites by additive techniques: from 30 to 90 wt.%. The study had purely fundamental character and was performed to check the feasibility of making such composites.

2. Materials and methods

The feedstock materials used for the manufacturing of the composite samples were two gas-atomized powders: tungsten carbide WC (LPW Technology Ltd.) and Inconel 625 (TLS Technik). WC powders were sieved to isolate powder particles of a specific size, 40 μm -125 μm for WC and 63 μm -106 μm for Inconel 625, which was confirmed by laser diffraction particle size analysis (IPS U, K μ K Instruments Ltd., Warsaw, Poland). The morphology, phase and chemical composition of each of the powders were investigated. Images of the powder morphology taken using an SEM (FEI Quanta 3D FEG, Fei) confirmed the spherical shape of the gas-atomized powders (Fig. 1).

SEM observation via BSE imaging of the WC powder revealed that the batch was a mixture of 4 types of particles appearing in the image as different shades of grey colour, shapes and sizes. The shades of grey in backscattered electron images can be related to the different mean atomic numbers of the elements present in investigated sample areas. The results of qualitative and semiquantitative energy dispersive X-ray spectroscopy (EDX) analyses of the WC powder particle types are shown in TABLE 1. Standardless quantitative EDS with ZAF correction was used, and presented results of chemical composition analysis have a semi-quantitative and comparative character.

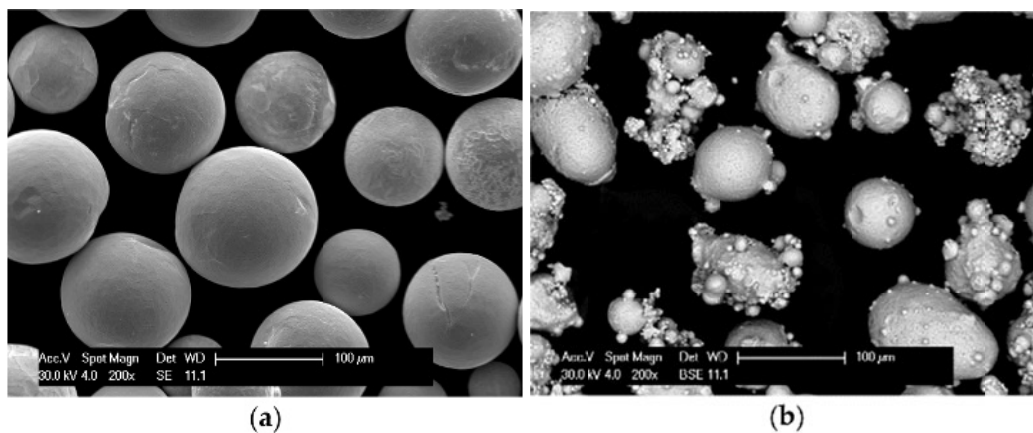


Fig. 1. Particle morphology of the powders used to produce composites by LENS additive technology: Inconel 625 (a) and commercial WC (b)

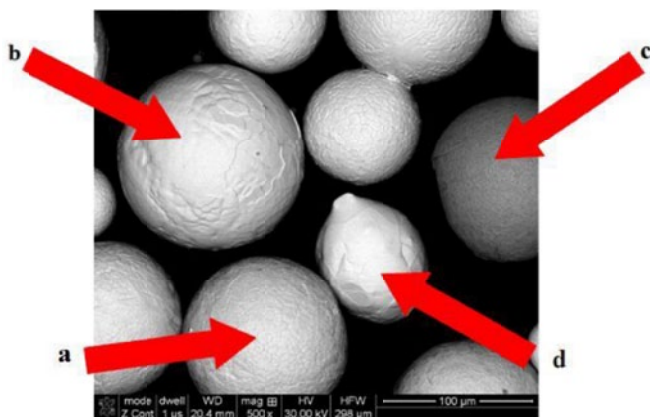


Fig. 2. Particles of commercial WC powder with different chemical compositions

TABLE 1

Chemical composition of the powder particles with the designations marked in Fig. 2. W – tungsten, C – carbon, WC, W₂C – intermetallic phases, (C) – solid solution of tungsten in carbon. * Semi-quantitative – due to the influence of the shape of the particles on the uncertainty of the quantitative analysis.

The results were given with 0.5% precision due to very high uncertainty of EDS in measurements of light elements (C) and when sample is not flat

| Element | Chemical composition* of selected particles | | | |
|---------|---|--------------------------|------------------|-----------|
| | a | b | c | d |
| | WC at.% | W ₂ C at.% | (C) + WC at.% | W at.% |
| W | 47.5 | 67.5 | 6.0 | 93.0 |
| C | 52.5 | 32.5 | 94.0 | 7.0 |

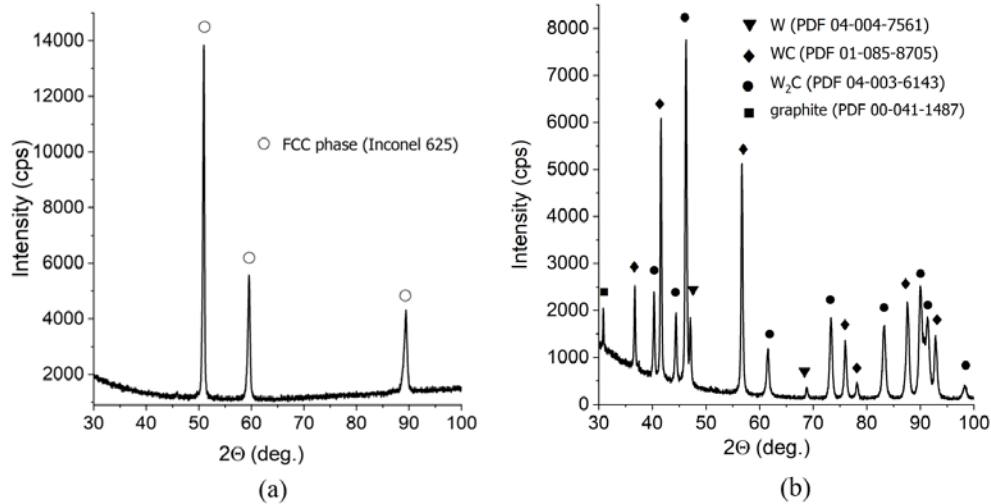


Fig. 3. Phase composition of Inconel 625 (a) and WC (b) powders used to produce composite samples

X-ray diffraction phase composition analysis (Rigaku ULTIMA IV, $\text{CoK}\alpha$, $\lambda = 1.79\text{\AA}$) confirmed that the WC powder was actually a mixture of tungsten, carbides ($\text{WC}+\text{W}_2\text{C}$) and, high carbon content particles composed likely of $\text{C}+\text{WC}$ mixture, as shown in Fig. 3a. For the Inconel 625 powder, the EDX chemical composition is characteristic of this alloy, and the XRD phase analysis confirmed that the powder particles were composed of a single FCC γ -Ni phase, as shown in Fig. 3b.

A laser engineered net shaping (LENS MR-7, Optomec, Inc.) machine equipped with a 500 W fiber laser was used to produce metal matrix composite samples. Fig. 4 shows a schematic view of the experimental setup. During laser forming, powders are fed into a melt pool that is produced by a focused laser beam with a power of 400 W and an effective beam diameter of 1 ± 0.05 mm. As the samples were built up layer by layer directly from CAD files on an Inconel 718 substrate, a key part of the process is controlling the thickness of the applied layers and the speed of the laser head, which were set to 0.4 mm and 10 mm/s, respectively. Twenty-four composite samples with base dimensions of 12×12 mm and assumed WC weight content in the range of ~ 30 -90% were made, and various heights were controlled by the number of layers applied. The compositions were made in-situ. Inconel and WC powders were fed from different powder feeders calibrated for this purpose. The designations

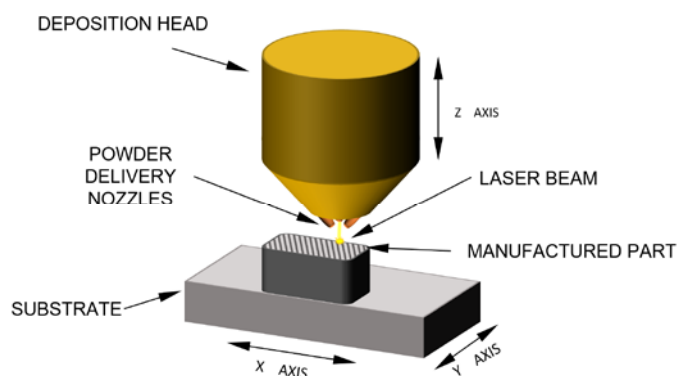


Fig. 4. Schematic of the LENS additive manufacturing process

of the produced samples are presented in TABLE 2. A Nikon MA 200 (Nikon Instruments) metallographic microscope was used to evaluate the microstructure of the produced LENS samples and to determine the amount of reinforcement in the matrix using the planimetric method, which is also presented in TABLE 2. The planimetric method enables an estimation of the weight share of a given phase in the alloy based on the relative volume of reinforcement in the matrix and its density. The uncertainty in estimating the surface and mass share of the reinforcing particles in the matrix is related to the partial dissolution of the reinforcing particles, especially in the remelted zones.

TABLE 2

Calculated reinforcement content in the matrix for produced samples

| Sample designation | Measured/calculated amount of reinforcement (wt.%) | Sample designation | Measured/calculated amount of reinforcement (wt.%) |
|--------------------|--|--------------------|--|
| 30_1 | 26.3 | 60_1 | 55.1 |
| 30_2 | 28.8 | 60_2 | 55.7 |
| 30_3 | 28.0 | 60_3 | 55.9 |
| 30_7 | 27.2 | 60_7 | 56.9 |
| 40_1 | 37.7 | 80_1 | 74.1 |
| 40_2 | 37.0 | 80_2 | 73.5 |
| 40_3 | 36.1 | 80_3 | 73.7 |
| 40_7 | 37.5 | 80_7 | 74.5 |
| 50_1 | 45.7 | 90_1 | 84.5 |
| 50_2 | 46.3 | 90_2 | 82.7 |
| 50_3 | 46.5 | 90_3 | 83.8 |
| 50_7 | 47.4 | 90_7 | 83.8 |

Samples for metallographic and microscopic analysis were prepared by mechanically grinding on sandpaper with gradations up to #4000 and polishing in diamond suspensions. The samples were cut perpendicular to the substrate. Macroscopic analysis of the produced samples was performed on a stereoscopic microscope at magnifications of $7.5\times$ and $10\times$ (NIKON SMZ1500). The microstructure and chemical composition of the produced

samples were characterized by scanning electron microscopy (SEM) with an energy-dispersive X-ray spectrometer. X-ray diffraction (XRD) phase analysis of the produced samples was performed on a Rigaku ULTIMA IV diffractometer using $\text{CoK}\alpha$ ($\lambda = 1.79 \text{ \AA}$) source (40 mA, 40 kV). Detex ultra linear detector was used. The phase identification was carried out using Rigaku PDXL software with PDF-4+ database. The HV10 hardness of the fabricated composite samples was determined using a Brinell-Vickers hardness tester (HPO 250).

3. Results and discussion

3.1. Macrostructure

The metallurgical quality of the fabricated samples was evaluated, with a focus on the presence of cracks. Fig. 5 and Fig. 6 show cross-sections of the produced samples from 30 to 90 wt.% of reinforcement on the example of samples produced during the 1-layer and 7-layer processes. The most favourable

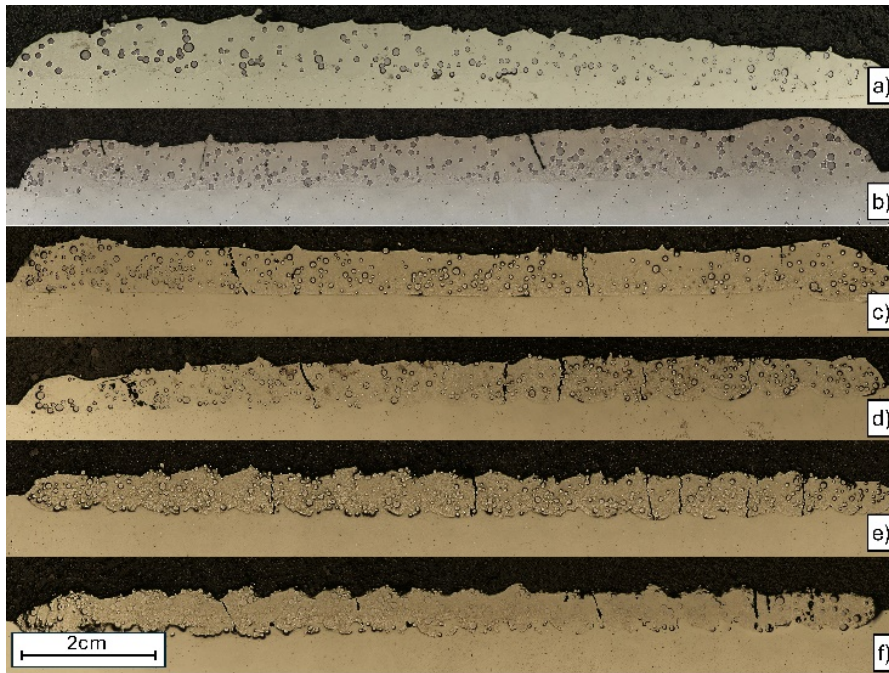


Fig. 5. Inconel 625-WC composite samples produced during the single layer process with different weight content of reinforcement: 30% (a), 40% (b), 50% (c), 60% (d), 80% (e), and 90% (f)

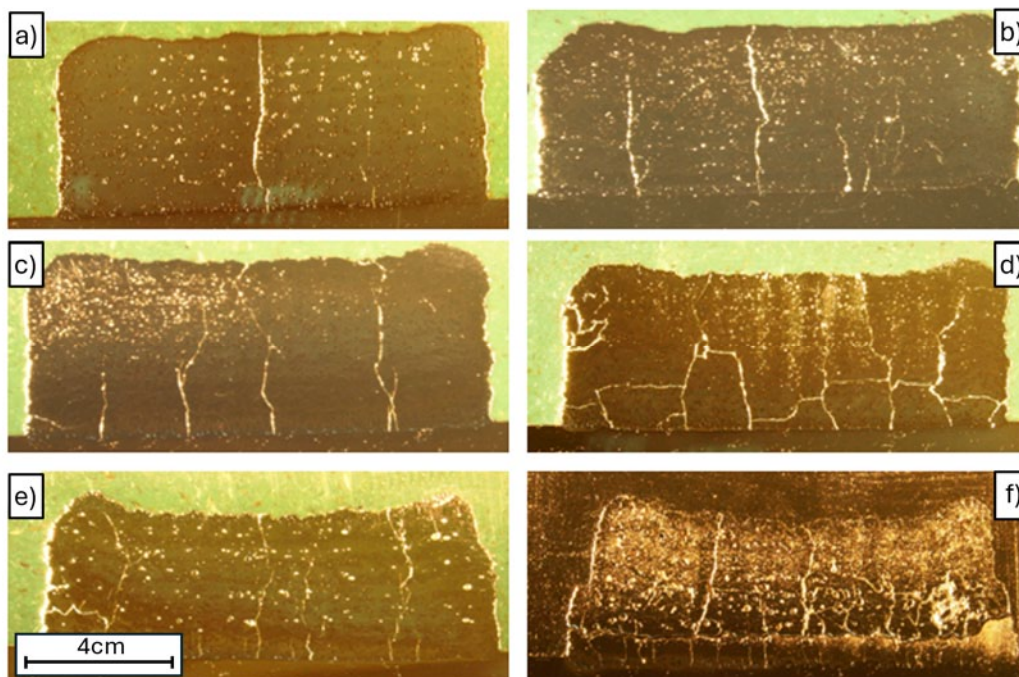


Fig. 6. Stereoscopic pictures Inconel 625-WC composite samples produced during the 7-layer process and the following contents (wt.%) of reinforcement: 30% (a), 40% (b), 50% (c), 60% (d), 80% (e), 90% (f)

mass content for WC reinforcement with respect to the applied manufacturing parameters is 30% in one layer, as increasing the number of layers and the number of reinforcement particles causes an increase in the number of thermal cracks, which run mainly perpendicular to the substrate. In the samples built up with 7 layers, where the share of reinforcement is 50% or more, macrocracks are observed both vertically to the substrate and in line with the laser scanning direction.

3.2. Microstructure

Microstructural analysis of the samples produced was carried out via optical and scanning electron microscopy. As it was already shown previously in Fig. 5, for the samples with different WC mass contents produced in one layer, the applied parameters of the manufacturing process allowed us to obtain dispersed spherical reinforcement as the WC powder particles did not melt. However, the distribution was not uniform regardless of the mass content of the reinforcement. In the direction perpendicular to the substrate, in the areas formed by overlapping of individual laser tracks, a certain volume of the reinforcement material is likely remelted.

Fig. 7 shows the microstructure of the fabricated composites with 30 to 90 wt.% WC in the Inconel 625 matrix at 500× magnification. As the share of reinforcement in the Inconel 625 dendritic matrix increases, the fraction of areas with W-rich dendrites around the reinforcement particles clearly increases, where the reaction between the matrix and reinforcement takes place. In addition, as a result of secondary scanning of the laser cladding coating, the remelted zones show refinement of the microstructure, as shown in the example of sample 30_7 in Fig. 8.

The surface distribution of elements, shown in Fig. 9, indicates that Cr, Ni and W are mainly segregated in the remelted zones. Refinement of the microstructure is often observed in alloys fabricated by the LENS® technique in the remelted and heat-affected regions on overlapping clad boundaries [15]. In Inconel 625-WC composites, these zones are described as areas of fine cellular grains [10].

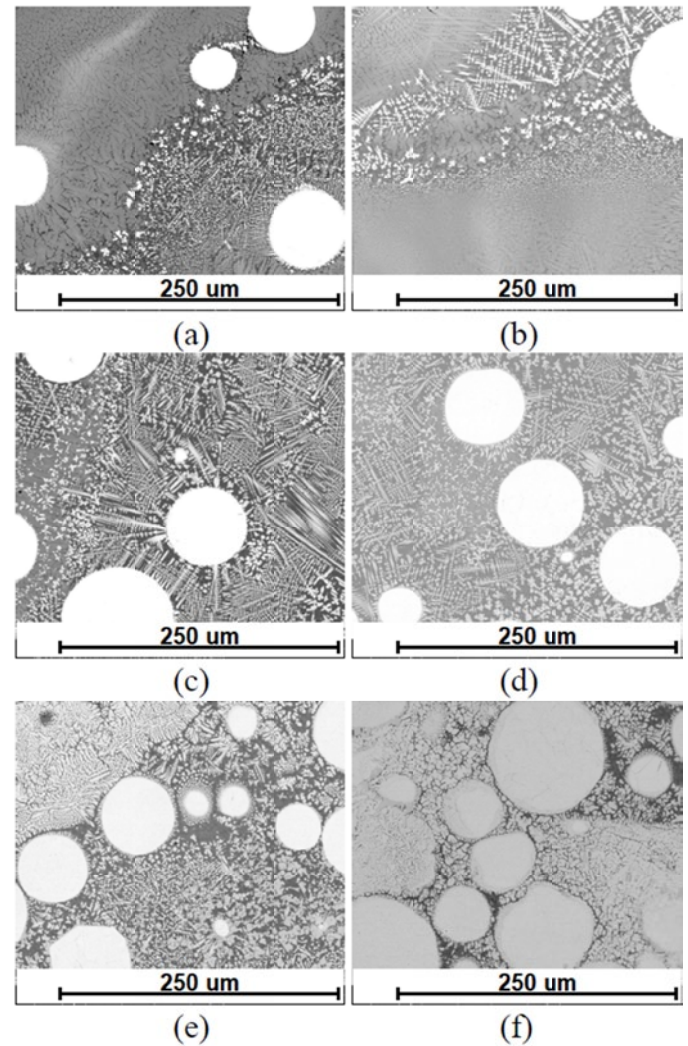


Fig. 7. Microstructure of Inconel 625-WC composite samples with the following content of reinforcement: 30% (a), 40% (b), 50% (c), 60% (d), 80% (e), and 90% (f)

Under higher magnification of the remelted areas (Fig. 8b), zones consisting of precipitates and eutectic regions can be observed (Fig. 8c). A similar eutectic microstructure was observed for Inconel 625-WC composites produced by laser cladding [9,16] and for Inconel 625-WC composites produced by laser

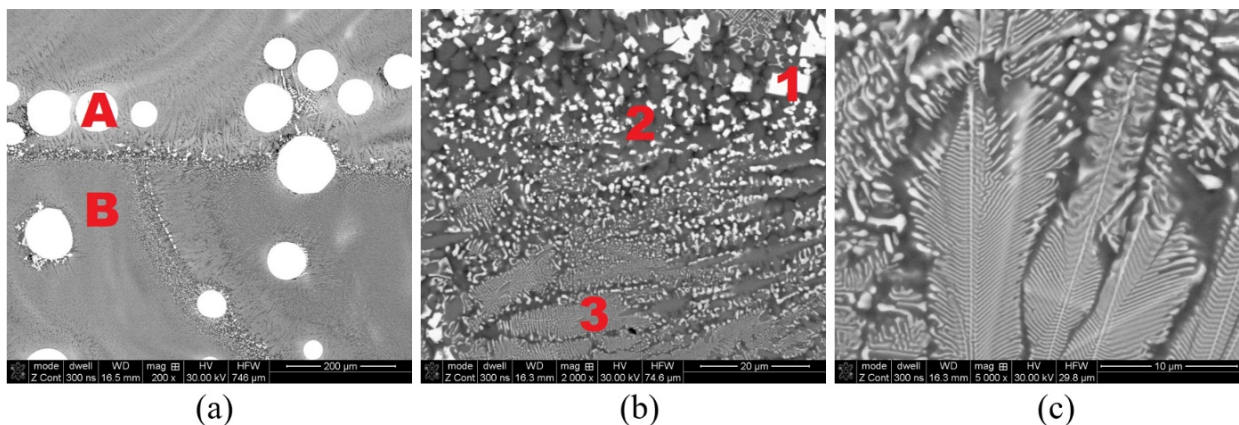


Fig. 8. Microstructure of the remelted and heat affected zone of sample 30_7

Chemical composition of areas marked with designations in Fig. 8

| Element | Chemical composition | | | | | | | | | |
|---------|----------------------|------|------|------|------|------|------|------|------|------|
| | A | | B | | 1 | | 2 | | 3 | |
| | wt.% | at.% | wt.% | at.% | wt.% | at.% | wt.% | at.% | wt.% | at.% |
| C | 0.4 | 5.3 | 0.3 | 1.8 | 0.3 | 2.3 | 0.2 | 1.1 | 0.3 | 1.4 |
| Nb | 0.0 | 0.0 | 2.8 | 2.1 | 3.4 | 3.3 | 1.5 | 1.0 | 2.3 | 1.7 |
| Mo | 1.5 | 2.5 | 7.6 | 5.4 | 12.7 | 12.1 | 4.6 | 3.1 | 7.7 | 5.5 |
| Cr | 1.7 | 4.9 | 17.8 | 23.2 | 11.9 | 21.0 | 17.9 | 22.0 | 16.5 | 21.9 |
| Fe | 0.3 | 0.7 | 0.4 | 0.5 | 0.2 | 0.4 | 0.5 | 0.5 | 0.4 | 0.5 |
| Ni | 3.4 | 8.8 | 52.0 | 60.0 | 23.9 | 37.2 | 62.3 | 67.8 | 51.9 | 61.0 |
| W | 92.8 | 77.7 | 19.2 | 7.1 | 47.6 | 23.7 | 13.0 | 4.5 | 21.0 | 7.9 |

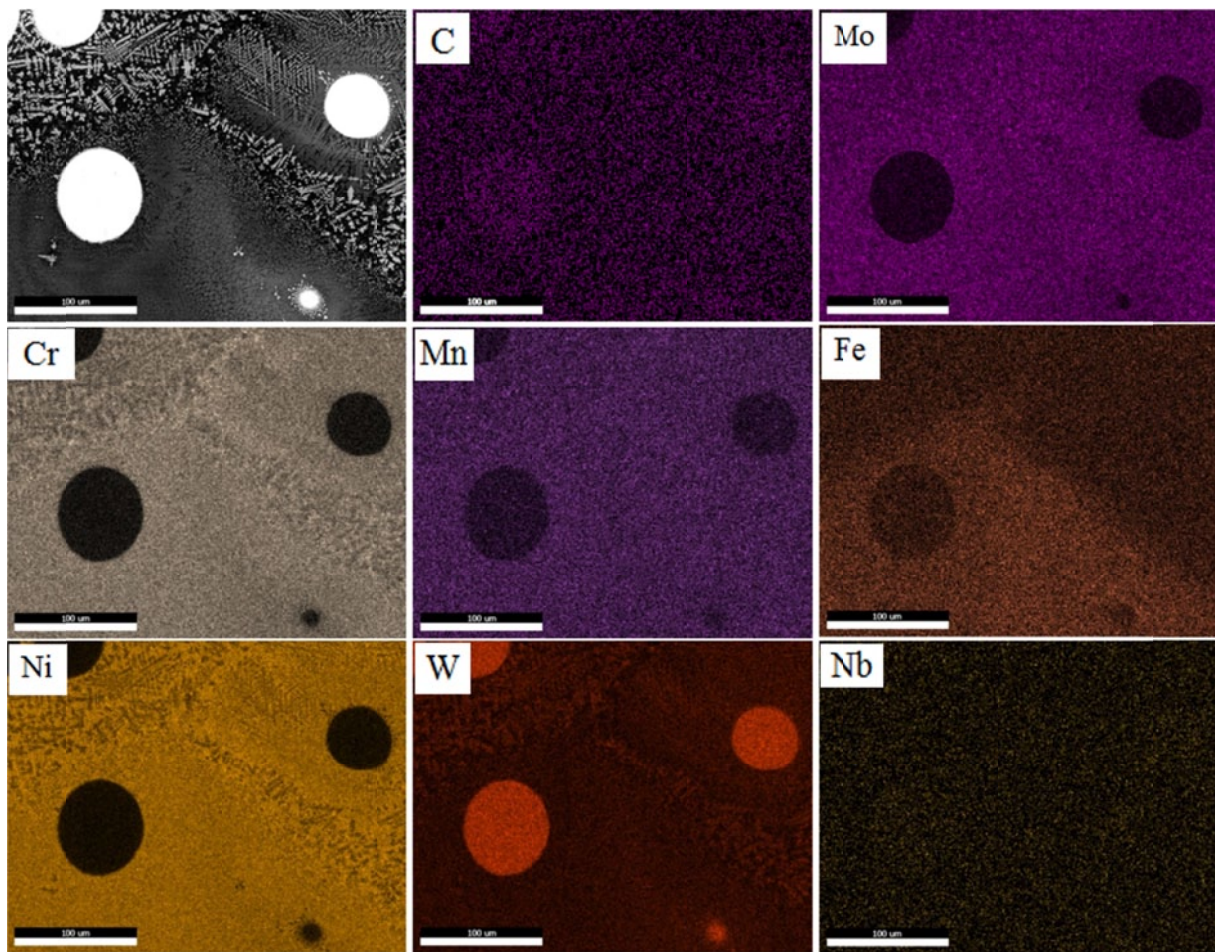


Fig. 9. Elemental mapping of the heat-affected area of sample 30_7

additive manufacturing [17]. The chemical compositions of the selected areas indicated in Fig. 8a and 8b are shown in TABLE 3. Notice that in Fig. 8a, the white spherical particle is almost pure W (area A), while in the matrix (area B), the dissolved amount of tungsten reaches approximately 7 at.%. In the remelted zones of the composite, (Ni,W)-rich precipitates are visible (area 1) that are also enriched in Cr in comparison to dark grey Ni-rich regions (area 2). According to the literature on Inconel 625-WC composites, in areas where remelting has occurred, the matrix around the precipitates contains dissolved carbon up to 44 at.%.

The secondary phases crystallizing as precipitates are carbides composed of tungsten, chromium and niobium [15]. A similar phenomenon was observed in composite coatings prepared by laser cladding containing up to 20 wt.% WC [18]. Area 3 is described in the literature as the γ -(Ni)/intermetallic eutectic region [15] or γ -(Ni) + carbide dendritic structures [16].

A microstructure typical for Inconel 625-WC composites fabricated by additive techniques is also observed in the produced samples but in the vicinity of reinforcement particles with chemical compositions corresponding to WC particles (as opposed

to particles of pure W). The overall chemical composition in the areas of this structure, as well as the surface contribution of areas differing in chemical composition, are presented in Fig. 10. WC reinforcement particles and an area with dendrites and precipitates in the remelted regions can be clearly observed. The chemical compositions of the areas distinguished by different colours are shown in TABLE 4.

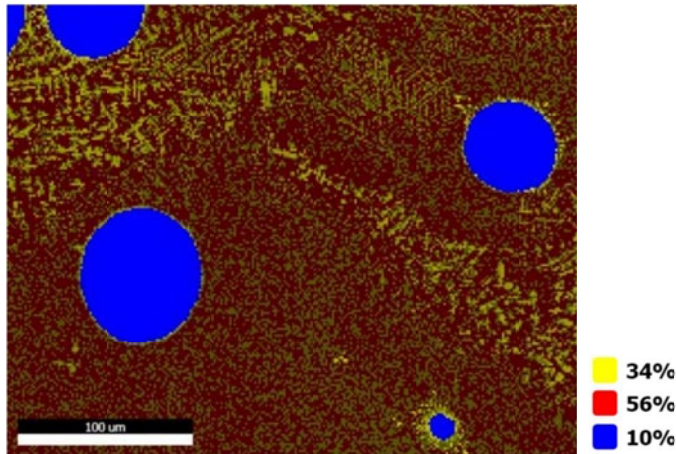


Fig. 10. Surface contribution of the phases present in the remelted areas

TABLE 4

Chemical composition of the areas marked in Fig. 10

| Element | Blue | | Red | | Yellow | |
|---------|------|------|------|------|--------|------|
| | wt.% | at.% | wt.% | at.% | wt.% | at.% |
| C | 6.2 | 42.6 | 3.6 | 17.6 | 4.4 | 22.2 |
| Mo | 1.1 | 0.9 | 3.8 | 2.3 | 5.2 | 3.3 |
| Cr | 3.7 | 6.0 | 16.2 | 18.1 | 16.2 | 18.9 |
| Nb | 0.6 | 0.9 | 0.9 | 1.0 | 0.9 | 1.0 |
| Fe | 1.0 | 1.5 | 1.8 | 1.9 | 1.8 | 2.0 |
| Ni | 8.6 | 12.1 | 51.8 | 51.3 | 39.7 | 40.9 |
| W | 77.5 | 34.9 | 18.6 | 5.9 | 27.5 | 9.0 |
| Nb | 1.4 | 1.2 | 3.4 | 2.1 | 4.3 | 2.8 |

The results of the XRD phase analysis of the produced samples are shown in Fig. 11. Phases found in the powders used to produce the specimens were identified; that is, WC, W_2C , FCC/Inconel 625. Additionally, unidentified strong Bragg peaks from unidentified phases for 30, 40 and 50% samples were found. The crystallographic database PDF4+ do not possess any phases that could be attributed to those peaks with possible elements. The phase component found in the commercial WC powder in the form of (C)+WC reacted with the Inconel 625 matrix and was no longer visible in the diffractograms of the produced composites. As expected, as the proportion of reinforcement increased, the Bragg peaks associated with the FCC phase Inconel 625 alloy disappeared, while the intensity of the reflections from the WC and W_2C phases increased. The relative contribution of these phases cannot be determined from the relative intensities of a particular reflection because even ignoring the possible crystallographic texture, the intensity of the X-ray reflection will be the result of a mixture of phases with different

mass X-ray absorption coefficients. All the allotropic phases of W_2C (α , β , γ) are metastable at room temperature; thus, the remaining phase strongly depends on the conditions of sample fabrication, such as the laser head feed rate or the width of the remelted areas.

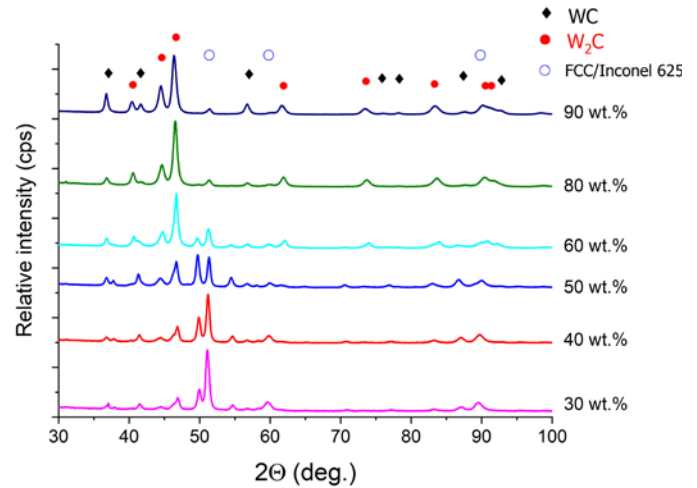


Fig. 11. XRD patterns of the additively manufactured Inconel 625-WC composite samples

3.3. Hardness measurements

Despite the presence of numerous stress cracks, it was possible to determine the hardness of the produced composites. The average values obtained from 10 measurements on each sample are shown in Fig. 12. As the reinforcement content in the matrix increases, the hardness of the composite increases almost linearly, considering that the hardness of laser additive-deposited Inconel 625 reaches 227 HV10 [19] and up to 402 HV10 after additional heat treatment [20]. The addition of 30% of reinforcement by weight increased the hardness of the composite by 2.5 times that of the Inconel 625 alloy.

With a 90 wt.% WC, the hardness of the composite was almost 6.5 times greater than that of the laser-deposited Inconel 625 and 5 times greater than that of the conventionally forged superalloy Inconel 625 [21]. Secondary phases formed in heat-affected and remelted areas were not observed in the XRD diffractograms of the produced samples due to their insignificant mass fraction.

A comparison of the results of the produced composite with a WC weight fraction of 30% with the results of the average HV0.2 and HV1 hardness of coatings of analogous composition, 470 HV0.2 [15] and 467 HV1 [22], respectively, revealed that a significantly greater value of the LENS® produced sample was obtained which was 625 HV10. The high hardness of the WC-Inconel 625 composites was attributed to the high microhardness within the eutectic regions composed of carbides and γ -(Ni) intermetallic phase and secondary phase precipitates in the form of carbides, up to 771 HV and 1194 HV, respectively [15], as well as to the (Ni,W)-rich precipitates and eutectic regions near the distance of the reinforcement particles composed of tungsten.

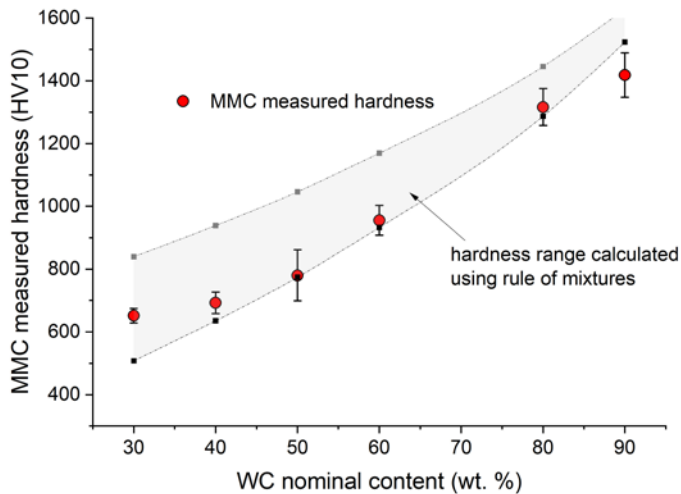


Fig. 12. The measured hardness of the produced MMC samples in the function of nominal reinforcement content. The grey field shows the expected hardness range calculated from rule of mixtures considering the different Inconel 625 hardness values after different heat treatments

4. Conclusions

A series of Inconel 625-WC metal matrix composite (MMC) samples were fabricated using the LENS® additive technique. In this study, an attempt was made to produce composites with a higher than described in the literature [13,17,20] reinforcement content (up to 90 wt.%), in the form of bulk samples – up to 7 layers of material. Samples produced using the LENS® technique exhibit discontinuities in their structure. The amount of cracks and spalling occurring in the samples increases with an increase in the number of layers produced and the amount of reinforcement in the matrix, however, the results of the laboratory tests and measurements carried out can be summarised as follows:

- 1) The technique used (LENS®) to produce the samples and the ability to calibrate the powder feeders enabled the manufacturing of MMC composites with a mass proportion of reinforcement close to the assumed amount.
- 2) Chemical and phase composition studies have shown that the spherical, gas-atomized commercial powder described as tungsten carbide is actually a mixture of WC, W₂C, (W) and (C)+WC particles. Therefore, in the produced samples, we observe remelted zones, which consist of both secondary phases of typical Inconel 625-WC metal matrix composites produced by additive methods (carbides as well as eutectics of carbides and γ -(Ni)-based phases) and carbide-free areas;
- 3) The higher hardness of the produced composites against single-layer specimens, as reported in the literature, is the result of a higher proportion of heat-affected and remelted zones as well as the precipitation processes of the intermetallic phases in these areas.
- 4) Optimization of the process (including heating of the substrate) may be possible to avoid or lower the cracking, however it is difficult to assume that crack-free samples might be produced for the highest reinforcement content.

Funding

This research was funded by the Military University of Technology UGB 22-809.

REFERENCES

- [1] V. Shankar, K.B.S. Rao, S. Mannan, Microstructure and mechanical properties of Inconel 625 superalloy. *J. Nucl. Mater.* **288**, 222-232 (2001). DOI: [https://doi.org/10.1016/S0022-3115\(00\)00723-6](https://doi.org/10.1016/S0022-3115(00)00723-6)
- [2] N. Khanna, K. Zadafiya, T. Patel, Y. Kaynak, R.A.R. Rashid, A. Vafadar, Review on machining of additively manufactured nickel and titanium alloys. *J. Mater. Res. Technol.* **15**, 3192-3221 (2021). DOI: <https://doi.org/10.1016/j.jmrt.2021.09.088>
- [3] A. Verma, A. Kapil, D. Klobčar, A. Sharma, A Review on Multiplicity in Multi-Material Additive Manufacturing: Process, Capability, Scale, and Structure. *Materials* **16**, 5246 (2023). DOI: <https://doi.org/10.3390/ma16155246>
- [4] D.E. Cooper, N. Blundell, S. Maggs, G.J. Gibbons, Additive layer manufacture of Inconel 625 metal matrix composites, reinforcement material evaluation. *J. Mater. Process. Technol.* **213** (12), 2191-2200 (2013). DOI: <https://doi.org/10.1016/j.jmatprotec.2013.06.021>
- [5] F. Zafar, O. Emadina, J. Conceição, M. Vieira, A. Reis, A Review on Direct Laser Deposition of Inconel 625 and Inconel 625-Based Composites – Challenges and Prospects. *Metals* **13**, 787 (2023). DOI: <https://doi.org/10.3390/met13040787>
- [6] J. Dutkiewicz, Ł. Rogal, D. Kalita, K. Berent, B. Antoszewski, H. Danielewski, M.S. Węglowski, M. Łazińska, T. Durejko, T. Czujko, Microstructure and Properties of Inconel 625 Fabricated Using Two Types of Laser Metal Deposition Methods. *Materials* **13**, 5050 (2020). DOI: <https://doi.org/10.3390/ma13215050>
- [7] L. Emanuelli, A. Molinari, M. Pellizzari, Interaction between WC and Inconel 625 under Solid and Liquid State Sintering Conditions. *Metals* **11**, 666 (2021). DOI: <https://doi.org/10.3390/met11040666>
- [8] S. Zhou, T. Xu, C. Hu, H. Wu, H. Liu, X. Ma, A comparative study of tungsten carbide and carbon nanotubes reinforced Inconel 625 composite coatings fabricated by laser cladding. *Opt. Laser Technol.* **140**, 106967 (2021). DOI: <https://doi.org/10.1016/j.optlastec.2021.106967>
- [9] E.O. Olakanmi, S.T. Nyadongo, K. Malikongwa, S.A. Lawal, A. Botes, S.L. Pityana, Multi-variable optimisation of the quality characteristics of fiber-laser clad Inconel-625 composite coatings. *Surf. Coat. Technol.* **357**, 289-303 (2019). DOI: <https://doi.org/10.1016/j.surfcoat.2018.09.063>
- [10] J. Huebner, P. Rutkowski, D. Kata, J. Kusiński, Microstructural and mechanical study of Inconel 625 – tungsten carbide composite coatings obtained by powder laser cladding. *Arch. Metall. Mater.* **62** (2), 531-538 (2017). DOI: <https://doi.org/10.1515/amm-2017-0078>

- [11] W. Li, R. Di, R. Yuan, H. Song, J. Lei, Microstructure, wear resistance and electrochemical properties of spherical/non-spherical WC reinforced Inconel 625 superalloy by laser melting deposition. *J. Manuf. Process.* **74**, 413-422 (2022). DOI: <https://doi.org/10.1016/j.jmapro.2021.12.045>
- [12] O. Ozgun, WC-Reinforced Inconel 625 Superalloy Matrix Composites. *IJST-T. Mech. Eng.* **44** (9), 825-839 (2020). DOI: <https://doi.org/10.1007/s40997-020-00357-6>
- [13] J. Huebner, D. Kata, J. Kusiński, P. Rutkowski, J. Lis, Microstructure of laser clad carbide reinforced Inconel 625 alloy for turbine blade application. *Ceram. Int.* **43** (12), 8677-8684 (2017). DOI: <https://doi.org/10.1016/j.ceramint.2017.03.194>
- [14] D. Janicki, High Power Diode Laser Cladding of Wear Resistant Metal Matrix Composite Coatings. *Solid State Phenom.* **199**, 587-592 (2013). DOI: <https://doi.org/10.4028/www.scientific.net/ssp.199.587>
- [15] N. Rońda, K. Grzelak, M. Polański, J. Dworecka-Wójcik, The Influence of Layer Thickness on the Microstructure and Mechanical Properties of M300 Maraging Steel Additively Manufactured by LENS® Technology. *Materials* **15**, 603 (2022). DOI: <https://doi.org/10.3390/ma15020603>
- [16] D. Janicki, M. Muszyfaga-Staszuk, Direct Diode Laser Cladding of Inconel 625/WC Composite Coatings. *J. Mech. Eng.* **62** (6), 343-372 (2016). DOI: <https://doi.org/10.5545/sv-jme.2015.3194>
- [17] J. Huebner, P. Rutkowski, A. Dębowska, D. Kata, Heating Conditions Influence on Solidification of Inconel 625-WC System for Additive Manufacturing. *Materials* **13**, 2932 (2020). DOI: <https://doi.org/10.3390/ma13132932>
- [18] Z.-H. Tian, Y.-T. Zhao, Y.-J. Jiang, H.-P. Ren, Microstructure and properties of Inconel 625 + WC composite coatings prepared by laser cladding. *Rare Met.* **40**, 2281-2291 (2020). DOI: <https://doi.org/10.1007/s12598-020-01507-0>
- [19] H. Danielewski, B. Antoszewski, Microstructure and Properties of Laser Additive Deposited of Nickel Base Super Alloy Inconel 625. *Arch. Foundry Eng.* **20** (3), 53-59 (2020). DOI: <https://doi.org/10.24425/afe.2020.133330>
- [20] B. Dubiel, K. Gola, S. Staroń et al., Effect of high temperature annealing on the microstructure evolution and hardness behavior of the Inconel 625 superalloy additively manufactured by laser powder bed fusion. *Archiv. Civ. Mech. Eng.* **23**, 249 (2023). DOI: <https://doi.org/10.1007/s43452-023-00787-4>
- [21] G. Wu, K. Ding, S. Qiao, T. Wei, X. Liu, Y. Gao, Weakening modes for the heat affected zone in Inconel 625 superalloy welded joints under different high temperature rupture conditions. *J. Mater. Res. Technol.* **14**, 2233-2242 (2021). DOI: <https://doi.org/10.1016/j.jmrt.2021.07.156>
- [22] K. Zhang, H. Ju, F. Xing, W. Wang, Q. Li, X. Yu, W. Liu, Microstructure and properties of composite coatings by laser cladding Inconel 625 and reinforced WC particles on non-magnetic steel. *Opt. Laser Technol.* **163**, 109321 (2023). DOI: <https://doi.org/10.1016/j.optlastec.2023.109321>
- [23] M. Li, K. Huang, X. Yi, Crack Formation Mechanisms and Control Methods of Laser Cladding Coatings: A Review. *Coatings* **13**, 1117 (2023). DOI: <https://doi.org/10.3390/coatings13061117>